Survival of Alpha and Intrinsically Photosensitive Retinal Ganglion Cells in NMDA-Induced Neurotoxicity and a Mouse Model of Normal Tension Glaucoma

Sari Honda,[1,2] Kazuhiko Namekata,[1] Atsuko Kimura,[1] Xiaoli Guo,[1] Chikako Harada,[1] Akira Murakami,[2] Akira Matsuda,[2] and Takayuki Harada[1]

[1]Visual Research Project, Tokyo Metropolitan Institute of Medical Science, Tokyo, Japan
[2]Department of Ophthalmology, Juntendo University Graduate School of Medicine, Tokyo, Japan

Correspondence: Kazuhiko Namekata, Visual Research Project, Tokyo Metropolitan Institute of Medical Science, 2-1-6 Kamikitazawa, Setagaya-ku, Tokyo 156-8506, Japan; namekata-kz@igakuken.or.jp.

Submitted: April 1, 2019
Accepted: July 31, 2019

Citation: Honda S, Namekata K, Kimura A, et al. Survival of alpha and intrinsically photosensitive retinal ganglion cells in NMDA-induced neurotoxicity and a mouse model of normal tension glaucoma. *Invest Ophthalmol Vis Sci*. 2019;60:3696–3707. https://doi.org/10.1167/iovs.19-27145

Purpose. We assess if α retinal ganglion cells (αRGCs) and intrinsically photosensitive retinal ganglion cells (ipRGCs) survive in mouse models of glaucoma.

Methods. Two microliters of *N*-methyl-D-aspartate (NMDA; 1 mM) or PBS were injected intraocularly 7 days before sacrifice. Immunohistochemical analyses of the retina were performed using antibodies against RNA-binding protein with multiple splicing (RBPMS), osteopontin, and melanopsin. Immunohistochemical analyses also were performed in adult mice with glutamate/aspartate transporter (GLAST) deletion (GLAST knockout [KO] mice), a mouse model of normal tension glaucoma.

Results. NMDA-induced loss of RBPMS-positive total RGCs was 58.4% ± 0.4% compared to PBS-treated controls, whereas the loss of osteopontin-positive αRGCs was 5.0% ± 0.6% and that of melanopsin-positive ipRGCs was 7.6% ± 1.6%. In GLAST KO mice, the loss of total RGCs was 48.4% ± 0.9% compared to wild-type mice, whereas the loss of αRGCs and ipRGCs was 3.9% ± 0.4% and 9.3% ± 0.5%, respectively. The distribution of survived total RGCs, αRGCs, and ipRGCs was similar regardless of the location of the retina.

Conclusions. These results suggest that αRGC and ipRGC are highly tolerant to NMDA-induced neurotoxicity and NTG-like neurodegeneration in GLAST KO mice.

Keywords: αRGC, ipRGC, neurodegeneration, glaucoma, cell tolerance

Glaucoma is the second leading cause of blindness in the world.[1,2] It is a neurodegenerative disease of the eye, which involves degeneration of retinal ganglion cells (RGCs) and optic nerve. In mammals, there are more than 40 different subtypes of RGCs that differ in soma size, morphology, dendrite arborization, and electrophysiologic functions.[3–6] For example, one of the first subtypes to be characterized was αRGCs.[7–9] αRGCs are identified by large cell bodies, wide and monostratified dendritic fields, and they are rich in proteins, including SMI32, osteopontin (OPN; *spp1*), and voltage-gated potassium channel subunit Kv6.4 (*kcng4*).[10–13] On the other hand, intrinsically photosensitive RGCs (ipRGCs) are the more recently identified subtype and these cells have important roles in nonimage forming vision, such as pupillary light reflexes and circadian rhythm.[14,15] ipRGCs express the photopigment melanopsin and are identified by their dendritic arbors stratifying in the sublaminae of the inner plexiform layer.[16,17] Recent studies have shown that αRGCs and ipRGCs may be highly tolerant to cell death and may have the capacity to regenerate after optic nerve injury.[11,18–20] Reports have indicated that function of ipRGCs is impaired in glaucoma patients,[21] and the density of melanopsin-expressing RGCs is reduced in severely staged glaucoma patients.[22] In rodents, brain derived neurotrophic factor (BDNF), which is a powerful neuroprotective agents for RGCs, rescues Brn3a-positive RGCs, but not melanopsin-positive RGCs in the ocular hypertension model.[23] In addition, ipRGCs show high resistance to optic nerve transection or crush, glutamate neurotoxicity, and acute ocular hypertension, but not to chronic ocular hypertension, suggesting that ipRGCs respond differently among injuries.[24–26]

Glaucoma usually is associated with increased IOP, but a subset of glaucoma presents with statistically normal IOP, called normal tension glaucoma (NTG), suggesting the possibility that non-IOP–dependent factors may contribute to the disease progression.[27,28] We previously reported that loss of glutamate/aspartate transporter (GLAST) in mice leads to progressive RGC loss and optic nerve degeneration while maintaining normal IOP, demonstrating key pathologic features of NTG.[29–31] Retinal degeneration in GLAST knockout (KO) mice may occur due to various factors, such as aging, glutamate neurotoxicity, and oxidative stress, which are important risk factors in human glaucoma.[32] Previous studies have reported that glaucoma patients show downregulation of glutamate transporters and glutathione levels,[33,34] suggesting that GLAST KO mice are useful as animal models of NTG.

RGC death also are experimentally induced by intravitreal injection of toxins, such as *N*-methyl-$_D$-aspartate (NMDA)[35,36] or staurosporine.[37] NMDA is a synthetic compound that selectively activates the NMDA subtype of glutamate receptors, and excessive activation of NMDA receptors induces a steep rise in intracellular calcium levels and causes excitotoxic cell death in neurons.[38,39] Glutamate excitotoxicity is thought to have important roles in RGC death in many retinal diseases, such as glaucoma, diabetic retinopathy, optic nerve injury, and

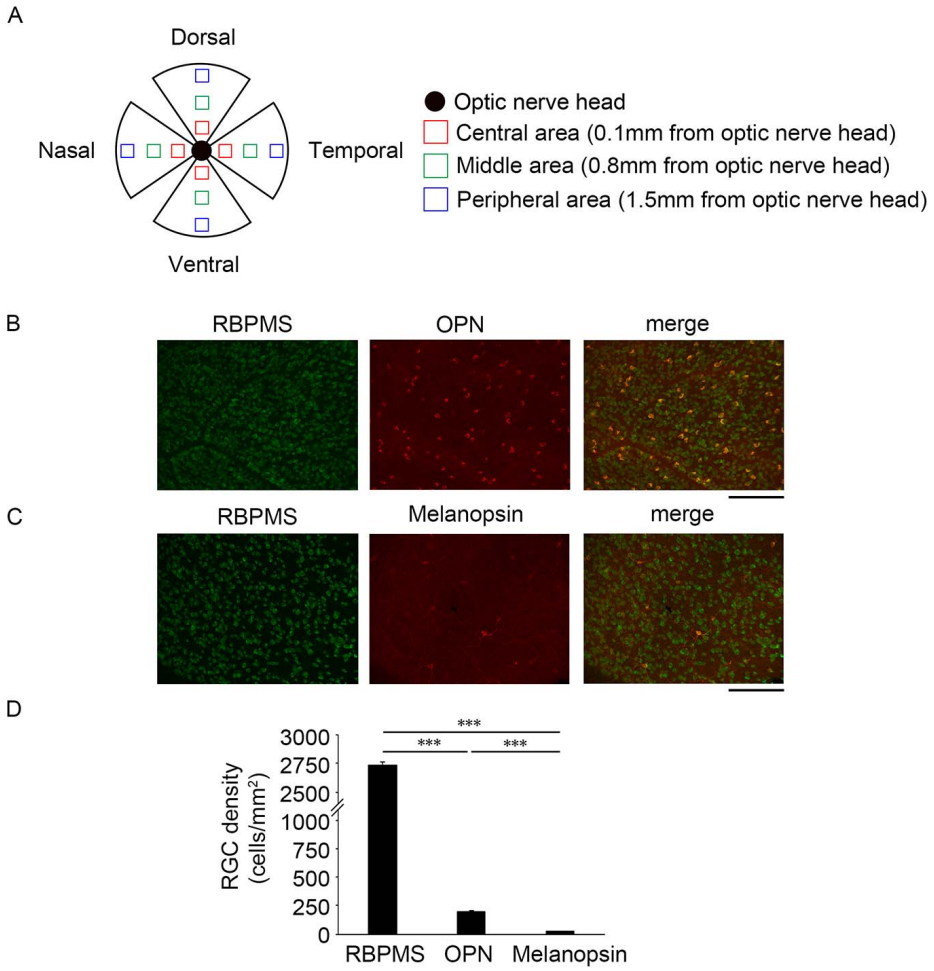

Figure 1. Immunostaining and quantification of total RGCs, αRGCs, and ipRGCs in the WT mouse retina. (**A**) Schematic illustration of the retinal area. (**B**, **C**) Immunohistochemical analysis of the flat-mounted WT mouse retina double-immunostained with anti-RBPMS antibody and anti-OPN antibodies (**B**), and with anti-RBPMS antibody and anti-melanopsin antibodies (**C**). These images were taken from the middle area. *Scale bar*: 200 μm. (**D**) Quantification of the RBPMS-, OPN-, and melanopsin-positive RGCs in (**B**, **C**). RGCs in the middle area of the dorsal, ventral, nasal, and temporal retina were counted and averaged. The data are represented as means ± SEM of six retinas. $^{***}P < 0.001$.

retinal ischemia.[32,39–42] Therefore, these experimentally-induced RGC death models are useful for exploring neuroprotective strategies that could lead to glaucoma therapy.[43,44] We examined αRGCs and ipRGCs to determine if there are any subtype-specific or region-specific responses to NMDA treatment or to NTG-like neurodegeneration in GLAST KO mice.

Materials and Methods

Mice

Experiments were performed using adult C57BL6 (wild type [WT]) and GLAST KO mice[30] on a C57BL6 background in accordance with the ARVO Statement for the Use of Animals in Ophthalmic and Vision Research. Animal experiments were approved by the institutional animal care and use committee of the Tokyo Metropolitan Institute of Medical Science (approval number TMiMS: 18041).

NMDA Administration

WT mice were deeply anesthetized with isoflurane (Intervet, Tokyo, Japan) and then received intravitreal injection of PBS or NMDA under a microsurgical microscope (Olympus, Tokyo, Japan) using a glass microsyringe with a 33-gauge needle (Ito Corporation, Shizuoka, Japan). Eyes were punctured at the upper temporal limbus and a volume of 2 μL PBS or NMDA (1 mM in PBS; Sigma-Aldrich Corp., St. Louis, MO, USA) was injected.[36,43] One week after injection, mice were sacrificed and the retinal samples were prepared for analysis.

Immunohistochemistry

Mice were sacrificed and perfused with 4% paraformaldehyde in 0.1 M phosphate buffer (pH 7.4). Eyes were enucleated, marked on the ear side so that they can be recognized as the temporal side of the retina. Eyes were postfixed in 4% paraformaldehyde for 2 hours at 4°C. Retinas then were isolated from the eyecup, incised radially into four radial pieces.

For immunolabeling with RNA-binding protein with multiple splicing (RBPMS) and OPN antibodies, the retinas were first incubated for 2 hours in a blocking solution containing 5% horse serum and 1% Triton X-100 in PBS (pH 7.4). The retinas then were incubated in a mixture of primary antibodies against RBPMS (1:1000; host, guinea-pig; ABN1376; Merck, Kenilworth, NJ, USA) and OPN (1:1000; host, goat; AF808-SP; R&D

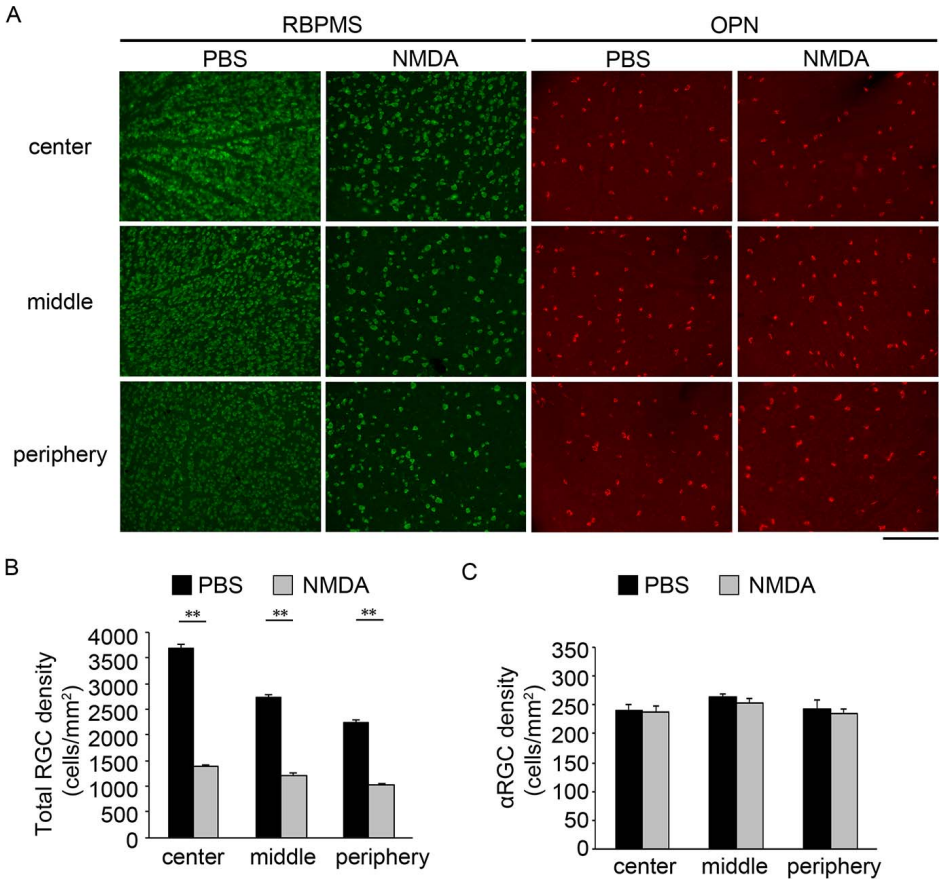

Figure 2. αRGCs survive after NMDA-induced neurotoxicity in mice regardless of the distance from the optic nerve head. (**A**) Immunostaining of the RBPMS-positive total RGCs and OPN-positive αRGCs in the central, middle, and peripheral areas of the retina in WT mice 7 days after intraocular injection of PBS or 1 mM NMDA. *Scale bar*: 200 μm. (**B**, **C**) Quantification of the RBPMS-positive (**B**) and OPN-positive (**C**) cell density in each area. The data are averaged cell density of the dorsal, ventral, nasal, and temporal regions, and represented as means ± SEM of six retinas for each experiment. $^{**}P < 0.01$.

Systems, Minneapolis, MN, USA) at 4°C for 2 days in a blocking solution. After washing three times in PBS, the samples were incubated with the appropriate secondary antibodies (for RBPMS, 1:1000; donkey anti-guinea pig Alexa Fluor 488; AB_2340472; Jackson Immuno Research Laboratories, West Grove, PA, USA; and for OPN, 1:1000; donkey anti-goat Alexa Fluor 568; A11057; Invitrogen, Waltham, MA, USA) in a blocking solution for 1 day.

For immunolabeling with RBPMS and melanopsin antibodies, the retinas were first incubated for overnight in a blocking solution containing 10% normal horse serum and 1% Triton X-100 in PBS (pH 7.4). The samples then were incubated with a mixture of primary antibodies against RBPMS (1:1000) and melanopsin (1:30000; host, rabbit; AB-N38; Advanced Targeting System, San Diego, CA, USA) at 4°C for 1 day in a blocking solution containing 1% normal horse serum and 1% Triton X-100 in PBS (pH 7.4). After washing three times in PBS, the samples were incubated in the appropriate secondary antibodies (for RBPMS, as described above, and for melanopsin, 1:1000; donkey anti-rabbit Alexa Fluor 647; ab150075; Abcam, Cambridge, UK) in a blocking solution containing 1% normal horse serum and 1% Triton X-100 in PBS (pH 7.4) for overnight 4°C.

Table 1. Density of RBPMS-Positive Cells in PBS-Treated Control and 1 mM NMDA-Treated Retinas

Region	Control (Cells/mm^2)	NMDA (Cells/mm^2)
Central	3692 ± 68	1391 ± 23*
Middle	2731 ± 44	1214 ± 36*
Peripheral	2243 ± 60	1016 ± 23*
Dorsal	3071 ± 95	1204 ± 16*
Ventral	2886 ± 72	1225 ± 9.0*
Nasal	2733 ± 63	1171 ± 16*
Temporal	2867 ± 42	1227 ± 4.1*

* $P < 0.01$.

Table 2. Density of OPN-Positive Cells in PBS-Treated Control and 1 mM NMDA-Treated Retinas

Region	Control (Cells/mm^2)	NMDA (Cells/mm^2)
Central	242 ± 11	238 ± 11*
Middle	263 ± 5.8	253 ± 8.3*
Peripheral	244 ± 14	234 ± 7.6*
Dorsal	256 ± 11	244 ± 2.6*
Ventral	253 ± 16	246 ± 6.9*
Nasal	254 ± 16	235 ± 8.1*
Temporal	250 ± 13	242 ± 2.2*

* Not statistically significant.

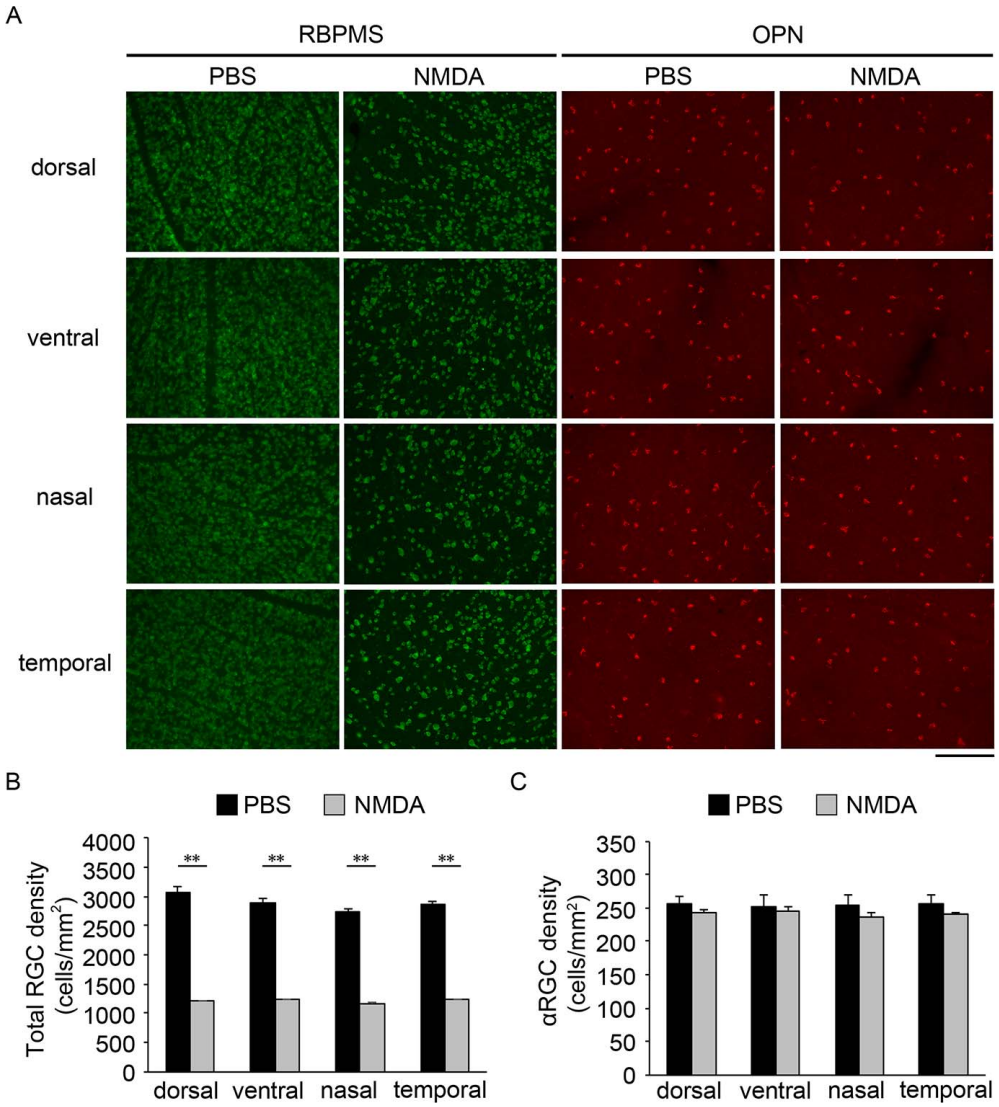

Figure 3. αRGCs survive after NMDA-induced neurotoxicity in mice regardless of the location of the retina. (**A**) Immunostaining of total RGCs and αRGCs in the middle areas from the dorsal, ventral, nasal, and temporal areas of the retina in WT mice 7 days after intraocular injection of PBS or 1 mM NMDA. *Scale bar*: 200 µm. (**B**, **C**) Quantification of the RBPMS-positive (**B**) and OPN-positive (**C**) cell density in each area. The data are averaged cell density of the central, middle and peripheral regions, and represented as means ± SEM of six retinas for each experiment. $^{**}P < 0.01$.

Histologic Analysis

The retinal whole mounts were examined with a fluorescence microscope (BZ-X800; Keyence, Osaka, Japan). The density of immunopositive RGCs was obtained from one central (0.1 mm from the optic disc), one middle (0.8 mm from the optic disc), and one peripheral (1.5 mm from the optic disc) areas (0.04 mm^2) per quadrant (dorsal, ventral, nasal, and temporal parts) of each retina. RGCs are counted manually by three people,

Table 3. Density of RBPMS-Positive Cells in WT and GLAST KO Retinas

Region	WT (Cells/mm^2)	GLAST KO (Cells/mm^2)
Central	3691 ± 67	1898 ± 51*
Middle	2725 ± 43	1418 ± 64*
Peripheral	2246 ± 62	1163 ± 84*
Dorsal	2878 ± 71	1413 ± 167*
Ventral	3068 ± 93	1472 ± 78*
Nasal	2881 ± 36	1625 ± 82*
Temporal	2722 ± 63	1461 ± 71*

* $P < 0.01$.

Table 4. Density of OPN-Positive Cells in WT and GLAST KO Retinas

Region	WT (Cells/mm^2)	GLAST KO (Cells/mm^2)
Central	265 ± 3.8	247 ± 6.9*
Middle	241 ± 11	238 ± 3.6*
Peripheral	257 ± 13	246 ± 4.5*
Dorsal	253 ± 14	256 ± 6.0*
Ventral	257 ± 12	242 ± 11*
Nasal	250 ± 14	232 ± 5.9*
Temporal	257 ± 16	244 ± 12*

* Not statistically significant.

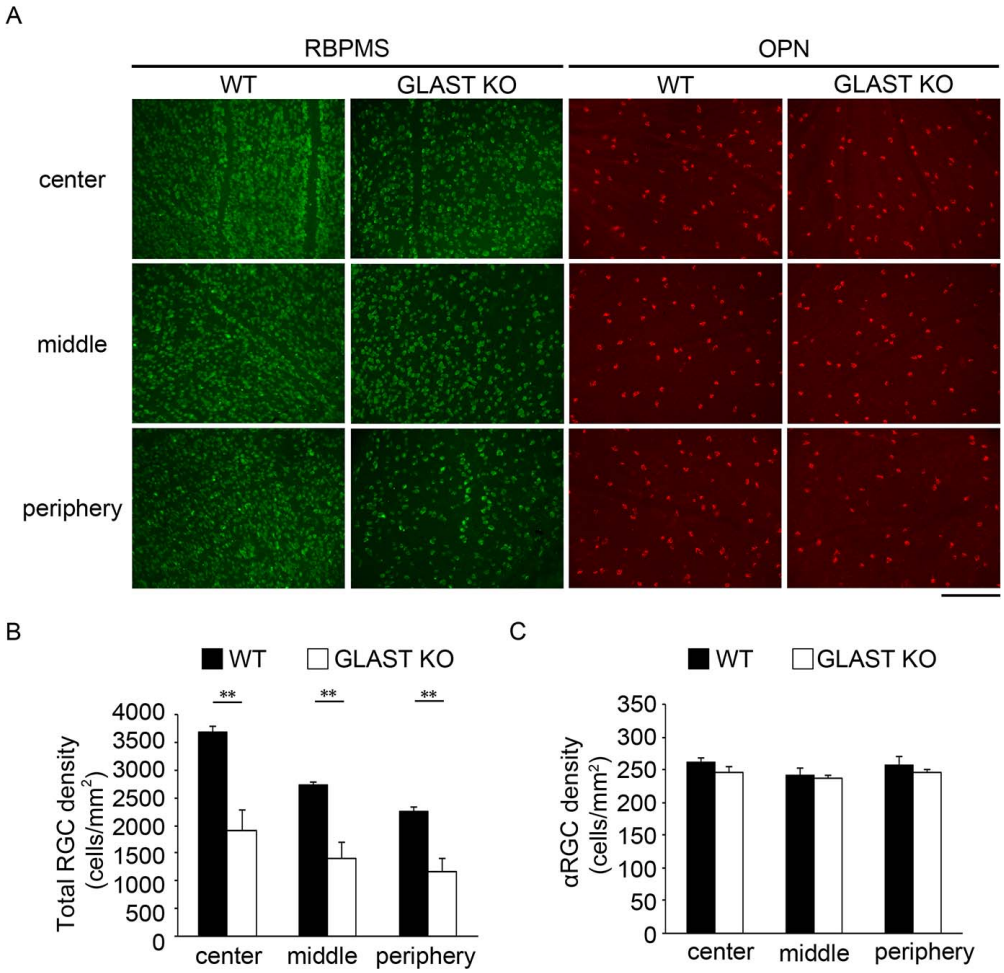

Figure 4. αRGCs survive in GLAST KO mice regardless of the distance from the optic nerve head. (**A**) Immunostaining of total RGCs and αRGCs in the central, middle and peripheral areas of the retina in WT and GLAST KO mice. *Scale bar*: 200 µm. (**B**, **C**) Quantification of the RBPMS-positive (**B**) and OPN-positive (**C**) cell density in each area. The data are averaged cell density of the dorsal, ventral, nasal, and temporal regions, and are represented as means ± SEM of six retinas for each experiment. $^{**}P < 0.01$.

blind to the treatments. The average density of RGCs per square millimeter was calculated.

Statistics

Data are represented as mean ± SEM. When statistical analyses were performed, the 1-way ANOVA followed by the Tukey's post hoc test was used. $P < 0.05$ was regarded as statistically significant. JMP version 13.1.0 (SAS Institute, Inc., Cary, NC, USA) was used for statistical analyses.

Results

Expression of OPN and Melanopsin in Mouse RGCs

To detect OPN-positive αRGCs and melanopsin-positive ipRGCs, we performed immunohistochemical analysis of the flat-mounted WT mouse retina with anti-RBPMS, anti-OPN, and anti-melanopsin antibodies. We divided the areas of the retina as shown in Figure 1A. Total RGCs were labeled with an anti-RBPMS antibody and some of them were double-labeled with an anti-OPN antibody (Fig. 1B). Melanopsin-positive ipRGCs

Table 5. Density of Melanopsin-Positive Cells in PBS-Treated Control and 1 mM NMDA-Treated Retinas

Region	Control (Cells/mm²)	NMDA (Cells/mm²)
Central	27 ± 1.8	24 ± 1.5*
Middle	27 ± 2.4	26 ± 1.1*
Peripheral	29 ± 0.9	26 ± 1.4*
Dorsal	29 ± 1.0	28 ± 1.8*
Ventral	27 ± 1.3	26 ± 1.8*
Nasal	28 ± 2.2	23 ± 1.5*
Temporal	27 ± 1.4	26 ± 1.9*

* Not statistically significant.

Table 6. Density of Melanopsin-Positive Cells in WT and GLAST KO Retinas

Region	WT (Cells/mm²)	GLAST KO (Cells/mm²)
Central	27 ± 2.4	24 ± 1.1*
Middle	28 ± 1.3	24 ± 1.1*
Peripheral	30 ± 1.0	26 ± 1.3*
Dorsal	30 ± 1.4	28 ± 1.6*
Ventral	27 ± 1.6	25 ± 1.2*
Nasal	28 ± 1.8	25 ± 1.6*
Temporal	28 ± 1.6	23 ± 1.0*

* Not statistically significant.

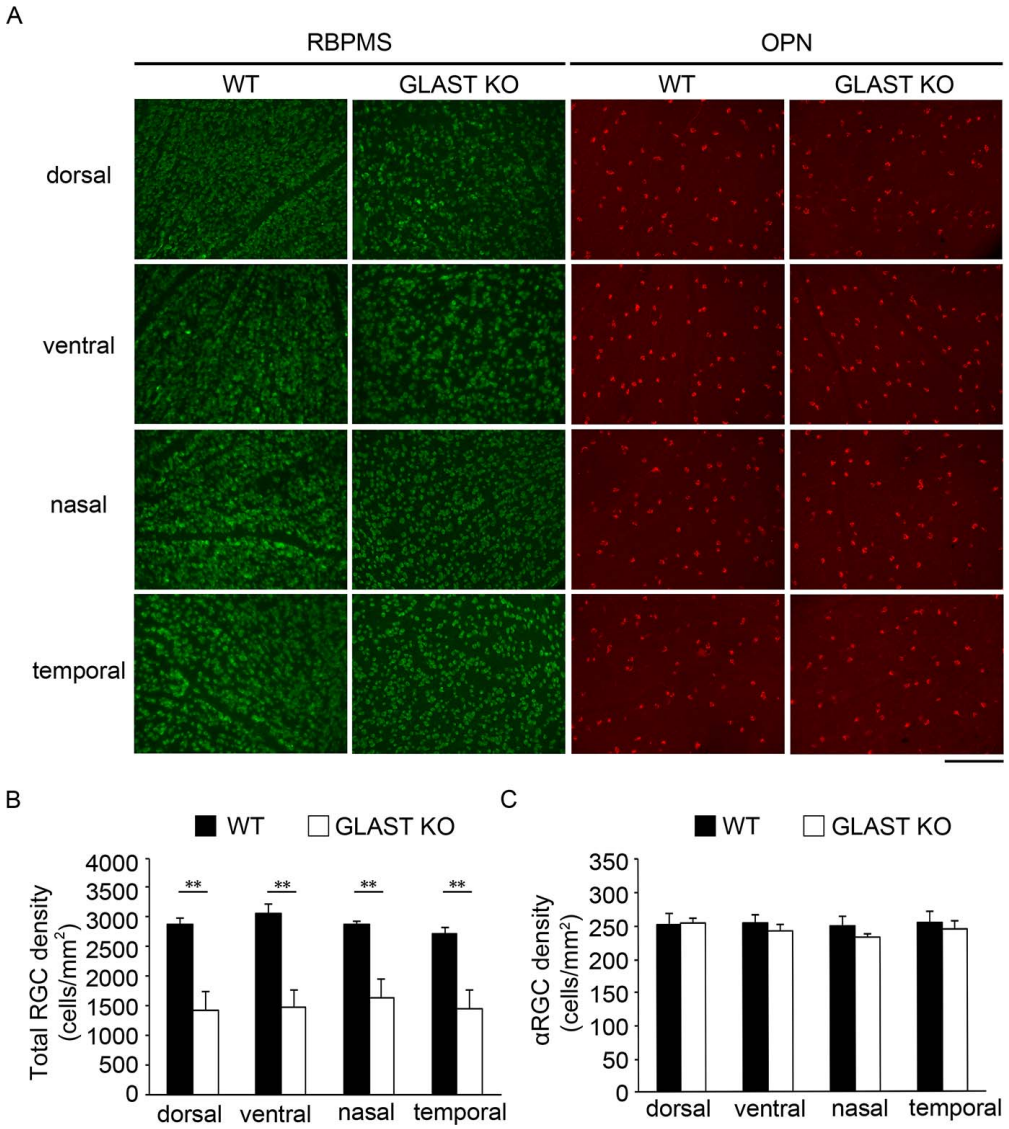

Figure 5. αRGCs survive in GLAST KO mice regardless of the location of the retina. (**A**) Immunostaining of total RGCs and αRGCs in the middle areas from the dorsal, ventral, nasal, and temporal areas of the retina in WT and GLAST KO mice. *Scale bar*: 200 µm. (**B**, **C**) Quantification of the RBPMS-positive (**B**) and OPN-positive (**C**) cell density in each area. The data are averaged cell density of the central, middle and peripheral regions, and are represented as means ± SEM of six retinas for each experiment. $^{**}P < 0.01$.

also were detected in some RBPMS-positive cells (Fig. 1C). Quantitative analysis in the middle areas of the dorsal, ventral, nasal, and temporal retina showed that the OPN- and melanopsin-positive RGCs were 8.9% ± 0.4% and 1.9% ± 0.4% of the RBPMS-positive cells, respectively (Fig. 1D). In our study, we did not detect many cells that were positive for OPN and melanopsin (Supplementary Fig. S1)

OPN-Positive αRGCs Survive After NMDA-Induced Neurotoxicity

To examine the survival rate of αRGCs following insult, we injected PBS or 1 mM of NMDA intraocularly to adult WT mice (6.1 ± 0.2 and 6.0 ± 0.3 months old, respectively) 7 days before sacrifice, and performed immunohistochemical analysis on the whole retina with anti-RBPMS and anti-OPN antibodies. As shown in representative images (Fig. 2A), NMDA significantly decreased the density of total RGCs in the central, middle, and peripheral areas (Fig. 2B). In contrast, the density of OPN-positive αRGCs was not decreased in the central, middle, or peripheral areas (Fig. 2C). We then performed similar quantitative analysis in four quadrants. As shown in representative images from the middle areas in each quadrant (Fig. 3A), NMDA significantly decreased the density in the dorsal, ventral, nasal, and temporal areas (Fig. 3B). In contrast, the density of OPN-positive αRGCs was not decreased in the dorsal, ventral, nasal, or temporal areas (Fig. 3C). The numeric data for the effects of NMDA on total RGCs and OPN-positive αRGCs are summarized in Tables 1 and 2.

In summary, NMDA-induced loss of RBPMS-positive total RGCs was 58.4% ± 0.4% compared to that of PBS-treated controls, whereas the loss of OPN-positive αRGCs was only 5.0% ± 0.6%. These results suggested that NMDA induces RGC death throughout the retina and αRGCs survive after NMDA-induced neurotoxicity regardless of the location of the retina.

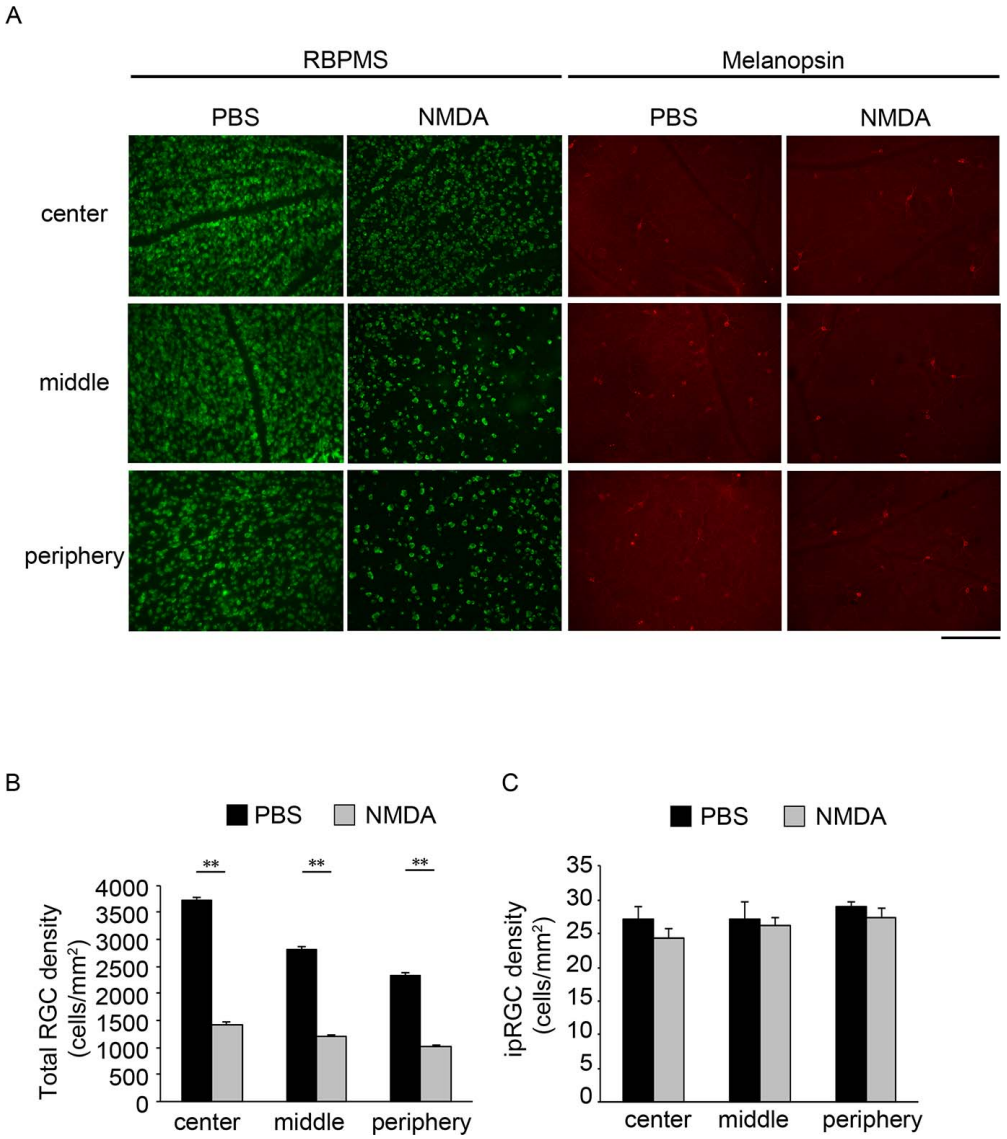

Figure 6. ipRGCs survive after NMDA-induced neurotoxicity regardless of the distance from the optic nerve head. (**A**) Immunostaining of total RGCs and ipRGCs in the central, middle, and peripheral areas of the retina in PBS or 1 mM NMDA-treated WT mice. *Scale bar*: 200 µm. (**B**, **C**) Quantification of the RBPMS-positive (**B**) and melanopsin-positive (**C**) cell density in each area. The data are averaged cell density of the dorsal, ventral, nasal, and temporal regions, and are represented as means ± SEM of six retinas for each experiment.

αRGCs Survive NTG-Like Retinal Degeneration in GLAST KO Mice

To examine the survival rate of αRGCs during NTG-like retinal degeneration, we performed immunohistochemical analysis with anti-RBPMS and anti-OPN antibodies in adult GLAST KO mice (7.1 ± 0.5 months old). As shown in representative images (Fig. 4A), the density of total RGCs in GLAST KO mice was significantly decreased in the central, middle, and peripheral areas compared to that of age-matched WT mice (6.5 ± 0.2 months old; Fig. 4B). In contrast, the density of OPN-positive αRGCs was not decreased in the central, middle, or peripheral areas (Fig. 4C). We then performed similar quantitative analysis in four quadrants. As shown in representative images from the middle areas in each quadrant (Fig. 5A), the density of total RGCs in GLAST KO mice was significantly decreased in the dorsal ,ventral, nasal, and temporal areas compared to WT mice (Fig. 5B). In contrast, the density of OPN-positive αRGCs was not decreased in these four areas (Fig. 5C). The numeric data for the total RGCs and OPN-positive αRGCs in GLAST KO mice are summarized in Tables 3 and 4.

In summary, in GLAST KO mice, the loss of total RGCs was 48.4% ± 0.9% compared to that of WT mice, whereas the loss of αRGCs was only 3.9% ± 0.4%. These results suggested that αRGCs survive NTG-like retinal degeneration in GLAST KO mice regardless of the location of the retina.

Melanopsin-Positive ipRGCs Survive After NMDA-Induced Neurotoxicity and in GLAST KO Mice

We next examined the survival rate of melanopsin-positive ipRGCs after NMDA injection and in GLAST KO mice. The density of ipRGCs after NMDA injection was not significantly decreased compared to that of PBS-treated control mice in the central, middle, and peripheral areas (Fig. 6). Similarly, the

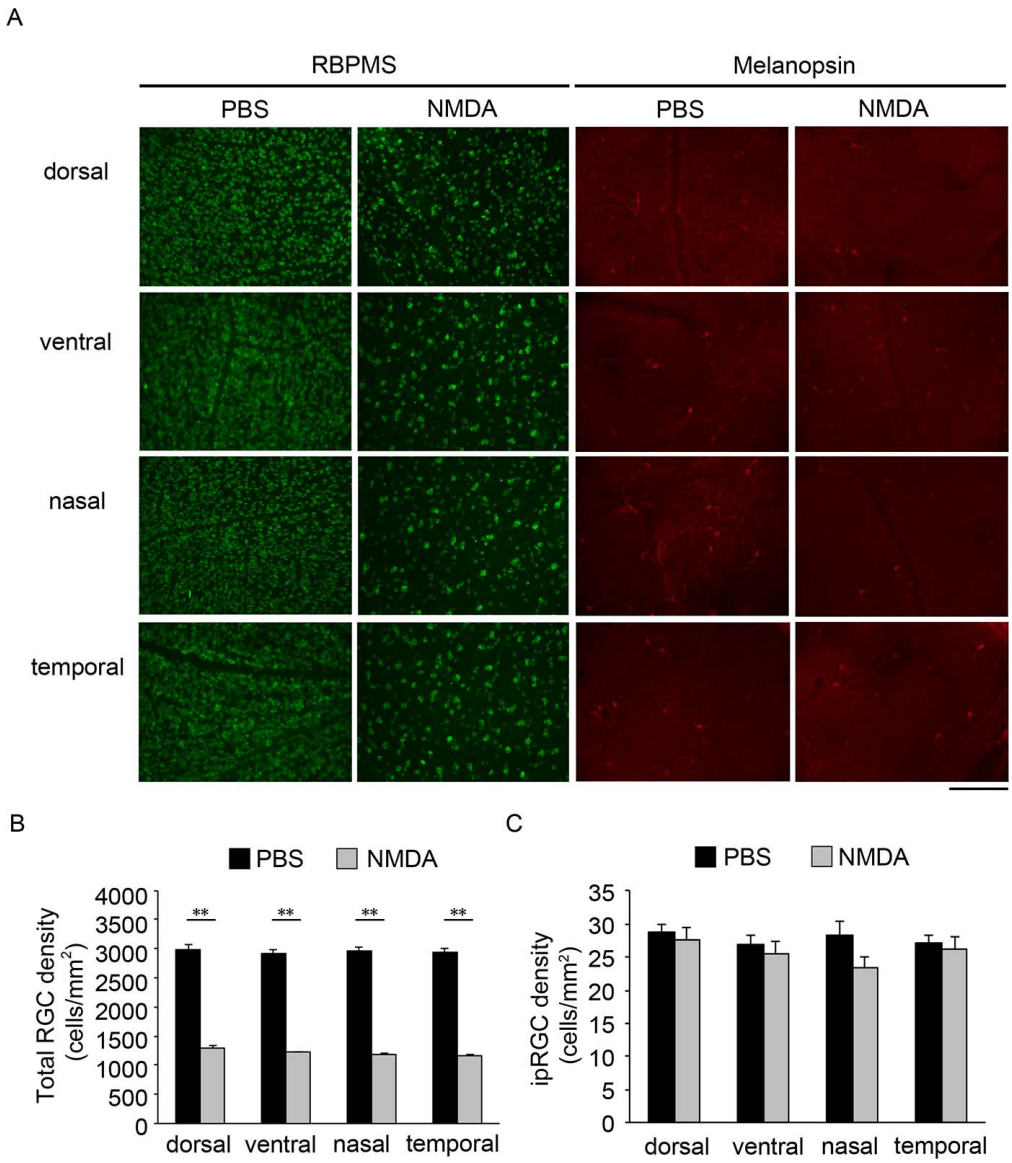

FIGURE 7. ipRGCs survive after NMDA-induced neurotoxicity regardless of the location of the retina. (**A**) Immunostaining of total RGCs and ipRGCs in the middle areas from the dorsal, ventral, nasal, and temporal areas of the retina in PBS or 1 mM NMDA-treated WT mice. *Scale bar*: 200 μm. (**B**) Quantification of the RBPMS-positive (**B**) and melanopsin-positive (**C**) cell density in each area. The data are averaged cell density of the central, middle, and peripheral regions, and are represented as means ± SEM of six retinas for each experiment.

density of ipRGCs after NMDA injection was not decreased compared to that of control mice in the dorsal, ventral, nasal, and temporal areas (Fig. 7). In GLAST KO mice, the density of ipRGCs in the central, middle, and peripheral areas was not significantly decreased compared to WT mice (Fig. 8). In addition, the density of ipRGCs in the dorsal, ventral, nasal, and temporal areas in GLAST KO mice was not decreased compared to WT mice (Fig. 9). The numeric data for the effects of NMDA on melanopsin-positive ipRGCs are summarized in Table 5, and for melanopsin-positive ipRGCs in GLAST KO mice are summarized in Table 6.

In summary, loss of melanopsin-positive ipRGCs was 7.6% ± 1.6% after NMDA neurotoxicity and 9.3% ± 0.5% in GLAST KO mice. The results suggested that ipRGCs survive after NMDA neurotoxicity and during NTG-like retinal degeneration in GLAST KO mice regardless of the location of the retina.

DISCUSSION

We showed that αRGCs and ipRGCs survive after NMDA-induced neurotoxicity and during NTG-like retinal degeneration in GLAST KO mice. We also examined whether there was any lesion specificity for the RGC loss, and found that αRGCs and ipRGCs survive regardless of the location of the retina. These results suggested that αRGCs and ipRGCs have high tolerance to IOP-independent pathogenic factors that may be involved in the progress of glaucoma.[32]

We showed that αRGCs and ipRGCs are tolerant to glutamate neurotoxicity. Our findings are supported by a recent study demonstrating that susceptibility of different types of genetically identified RGCs to NMDA excitotoxicity varies significantly, and that αRGCs are the most resistant RGCs to NMDA excitotoxicity.[45] Currently, the mechanisms that explain their high survival rate under the toxic environment in

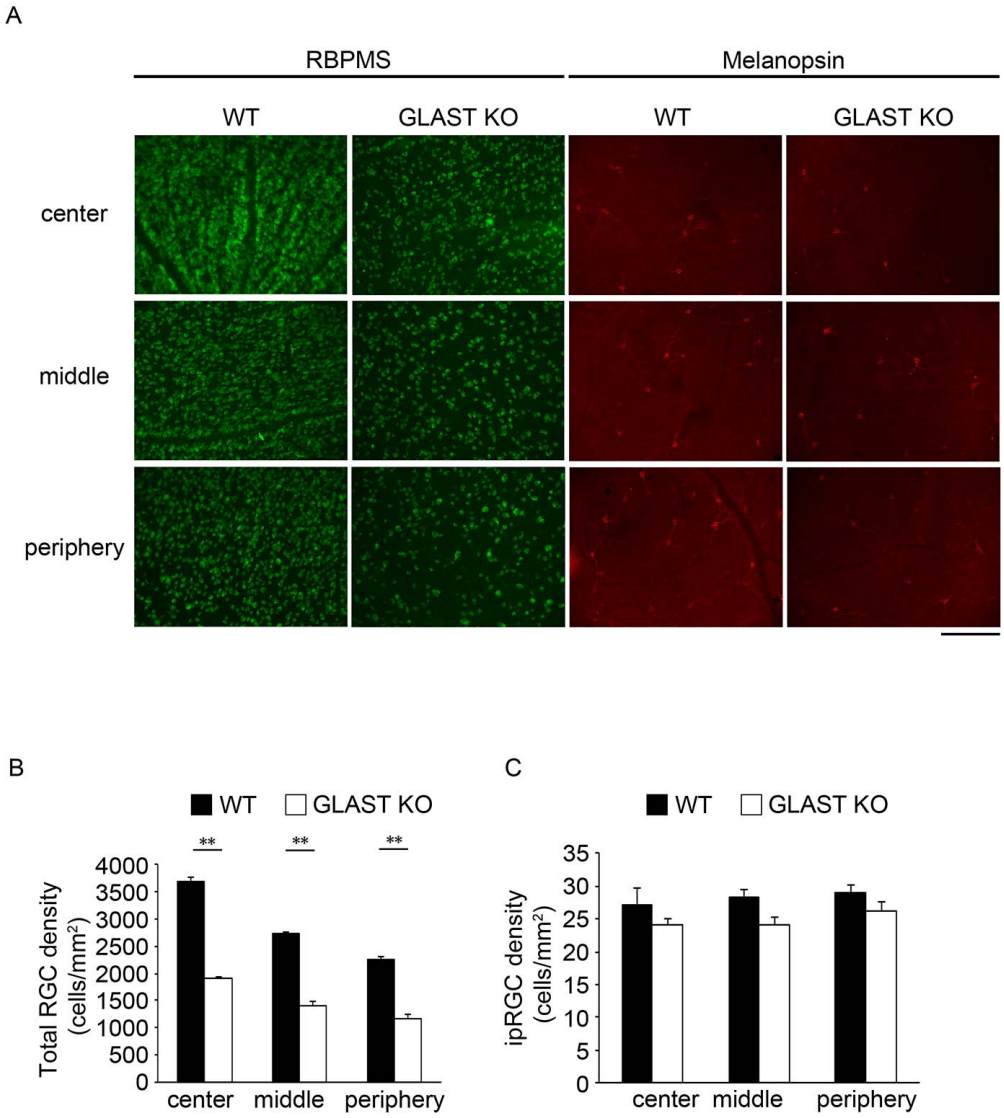

Figure 8. ipRGCs survive in GLAST KO mice regardless of the distance from the optic nerve head. (**A**) Immunostaining of total RGCs and ipRGCs in the central, middle, and peripheral areas of the retina in WT and GLAST KO mice. *Scale bar*: 200 µm. (**B**, **C**) Quantification of the RBPMS-positive (**B**) and melanopsin-positive (**C**) cell density in each area. The data are averaged cell density of the dorsal, ventral, nasal, and temporal regions, and are represented as means ± SEM of six retinas for each experiment.

our models are unknown; although, some studies suggest a role of dopaminergic amacrine cells for protection of ipRGCs in NMDA-induced retinal injury.[46–48] Other studies have reported that αRGCs and ipRGCs are tolerant to optic nerve injury, and one explanation for this may be their high mTOR activity.[11,18,49,50] Therefore, future studies may focus on identifying the survival mechanisms in these two RGC subtypes. Furthermore, overexpression of OPN or melanopsin in RGCs boosts mTOR signaling to promote axon regeneration.[11,51] These data suggest that understanding the neuroprotective and neuroregenerative mechanisms in αRGCs and ipRGCs and overexpression of relevant key genes to non-αRGCs and non-ipRGCs may be an effective therapeutic strategy for neurodegenerative diseases, such as glaucoma.

In our study, the distribution of αRGCs and ipRGCs was similar, and the survival rate of these RGCs also was similar regardless of the location of the retina. Our results are in agreement with previous studies showing that under normal conditions, cells positive for SMI-32 (αRGCs) and the melanopsin fluorescent reporter (ipRGCs) were distributed evenly throughout the mouse retina,[52] and that the ratios of ipRGC in the peripheral, paracentral, and central retinal regions were consistent in the fully-developed Sprague Dawley rat retina, in which immunotoxin induced uniform cell lesioning across the entire retina.[53] However, some reports indicate that ipRGC distribution is asymmetrical and that they are more abundant in the superior or dorsal retina.[15,54,55] We cannot explain the reason for this discrepancy, but it is possible that the use of low concentration of the melanopsin antibody may have contributed to the difference. In our study, we did not detect any statistically significant differences in the surviving ipRGCs as well as αRGCs in each retinal region in the NMDA-treated and GLAST KO mouse retina. It would be interesting to find if αRGCs and ipRGCs survive in the human glaucoma retina and if their localization shows regional specificity.

Fascinatingly, ipRGC responses and function are impaired in glaucoma patients causing smaller post-illumination pupil response (PIPR) and reduced sleep quality.[56–59] One study suggests that glaucoma patients show "disturbed synaptic function and altered interaction between photoreceptors,

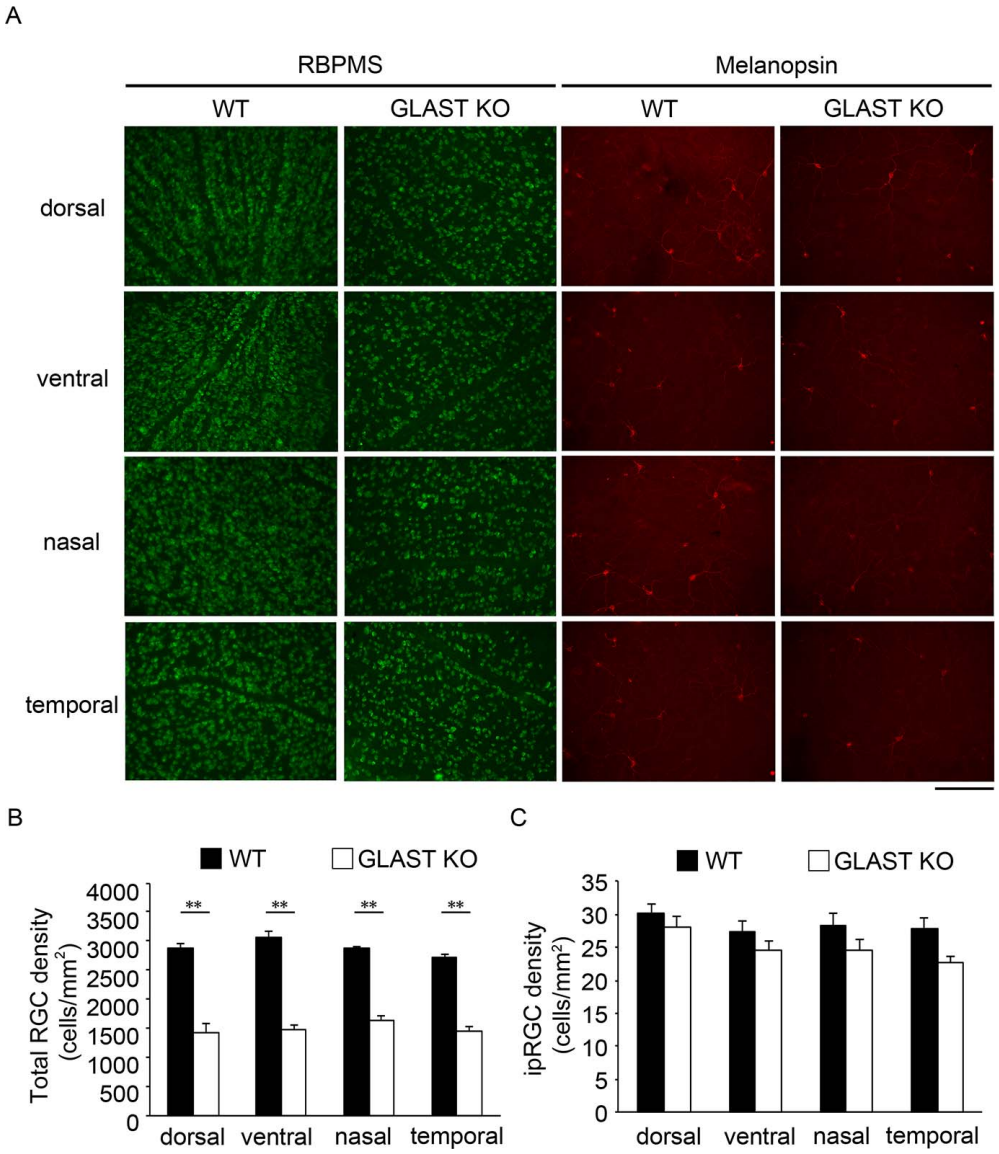

FIGURE 9. ipRGCs survive in GLAST KO mice regardless of the location of the retina. (**A**) Immunostaining of total RGCs and ipRGCs in the middle areas from the dorsal, ventral, nasal, and temporal areas of the retina in WT and GLAST KO mice. *Scale bar*: 200 µm. (**B**, **C**) Quantification of the RBPMS-positive (**B**) and melanopsin-positive (**C**) cell density in each area. The data are averaged cell density of the central, middle and peripheral regions, and are represented as means ± SEM of six retinas for each experiment.

RGCs, and ipRGCs.[60] Together with our data that demonstrate the high survival rate of ipRGCs in glaucoma models, one may speculate that the cells are not dead, but synaptic connections are disturbed in glaucoma patients. In such case, in which retraction of dendrites and/or axons is partly causing visual impairment in addition to RGC death, promoting dendrite or axon regeneration and reforming synapses could restore neuronal connections and lead to partial recovery of sight. If this is possible, there is a hope for glaucoma patients to improve their vision while preventing or slowing down disease progression with conventional therapy. Future studies will include investigations into the synaptic connections in glaucoma models.

We used GLAST KO mice as an animal model of NTG. This model closely mimics pathology of NTG, including RGC loss, optic nerve atrophy, and visual impairment while maintaining normal IOP.[30,31] However, some glaucomatous features are not observed in GLAST KO mice. For example, the RGC loss in these mice is not restricted to specific regions as seen in human glaucoma, and the onset of retinal degeneration occurs not in aged mice, but in young mice (3 weeks of age). The early onset of disease may be an advantage as this allows obtaining experimental results speedily and GLAST KO mice have been providing useful information regarding NTG therapy.[31,36,61,62] Survival of αRGCs and ipRGCs in GLAST KO mice may provide an experimental platform for examining selective vulnerability of RGCs in NTG-like degeneration, which could lead to a new therapy.

In summary, our findings suggested that αRGC and ipRGC are highly tolerant to NMDA neurotoxicity and glaucoma-like retinal degeneration in GLAST KO mice. Although the roles of αRGCs and ipRGCs in glaucoma have not been fully elucidated yet, further studies to elucidate the reasons for this high tolerance and the detailed survival mechanisms of αRGCs and ipRGCs, for example, determination of factors that are common to resilient RGCs, may lead to devising a new therapeutic approach for glaucoma.

Acknowledgments

The authors thank Mayumi Kunitomo, Keiko Okabe, and Sayaka Ihara for their technical assistance.

Supported in part by JSPS KAKENHI Grants-in-Aid for Scientific Research JP16K08635 (KN), JP17K07123 (AK), JP16K07076 (XG), JP19K09943 (CH), JP16K11303 (AM), JP18K19625 (TH), the Taiju Life Social Welfare Foundation, and the Takeda Science Foundation (TH).

Disclosure: **S. Honda**, None; **K. Namekata**, None; **A. Kimura**, None; **X. Guo**, None; **C. Harada**, None; **A. Murakami**, None; **A. Matsuda**, None; **T. Harada**, None

References

1. Resnikoff S, Pascolini D, Etya'ale D, et al. Global data on visual impairment in the year 2002. *Bull World Health Organ*. 2004; 82:844–851.
2. Pascolini D, Mariotti SP. Global estimates of visual impairment: 2010. *Br J Ophthalmol*. 2012;96:614–618.
3. Masland RH. The neuronal organization of the retina. *Neuron*. 2012;76:266–280.
4. Sanes JR, Masland RH. The types of retinal ganglion cells: current status and implications for neuronal classification. *Annu Rev Neurosci*. 2015;38:221–246.
5. Rheaume BA, Jereen A, Bolisetty M, et al. Single cell transcriptome profiling of retinal ganglion cells identifies cellular subtypes. *Nat Commun*. 2018;9:2759.
6. Baden T, Berens P, Franke K, Roman Roson M, Bethge M, Euler T. The functional diversity of retinal ganglion cells in the mouse. *Nature*. 2016;529:345–350.
7. Boycott BB, Wassle H. The morphological types of ganglion cells of the domestic cat's retina. *J Physiol*. 1974;240:397–419.
8. Cleland BG, Levick WR, Wassle H. Physiological identification of a morphological class of cat retinal ganglion cells. *J Physiol*. 1975;248:151–171.
9. Wassle H, Peichl L, Boycott BB. Morphology and topography of on- and off-alpha cells in the cat retina. *Proc R Soc Lond B Biol Sci*. 1981;212:157–175.
10. Peichl L. Alpha ganglion cells in mammalian retinae: common properties, species differences, and some comments on other ganglion cells. *Vis Neurosci*. 1991;7:155–169.
11. Duan X, Qiao M, Bei F, Kim IJ, He Z, Sanes JR. Subtype-specific regeneration of retinal ganglion cells following axotomy: effects of osteopontin and mTOR signaling. *Neuron*. 2015;85: 1244–1256.
12. Krieger B, Qiao M, Rousso DL, Sanes JR, Meister M. Four alpha ganglion cell types in mouse retina: function, structure, and molecular signatures. *PLoS One*. 2017;12:e0180091.
13. Berson DM. Retinal ganglion cell types and their central projections. In: *The Senses: A Comprehensive Reference.* Vol. 1. New York: Academic Press; 2008:491–519.
14. Berson DM, Dunn FA, Takao M. Phototransduction by retinal ganglion cells that set the circadian clock. *Science*. 2002;295: 1070–1073.
15. Hattar S, Liao HW, Takao M, Berson DM, Yau KW. Melanopsin-containing retinal ganglion cells: architecture, projections, and intrinsic photosensitivity. *Science*. 2002; 295:1065–1070.
16. Ecker JL, Dumitrescu ON, Wong KY, et al. Melanopsin-expressing retinal ganglion-cell photoreceptors: cellular diversity and role in pattern vision. *Neuron*. 2010;67:49–60.
17. Berson DM, Castrucci AM, Provencio I. Morphology and mosaics of melanopsin-expressing retinal ganglion cell types in mice. *J Comp Neurol*. 2010;518:2405–2422.
18. Daniel S, Clark AF, McDowell CM. Subtype-specific response of retinal ganglion cells to optic nerve crush. *Cell Death Discov*. 2018;4:7.
19. Sanchez-Migallon MC, Valiente-Soriano FJ, Nadal-Nicolas FM, Di Pierdomenico J, Vidal-Sanz M, Agudo-Barriuso M. Survival of melanopsin expressing retinal ganglion cells long term after optic nerve trauma in mice. *Exp Eye Res*. 2018;174:93–97.
20. Nadal-Nicolas FM, Sobrado-Calvo P, Jimenez-Lopez M, Vidal-Sanz M, Agudo-Barriuso M. Long-term effect of optic nerve axotomy on the retinal ganglion cell layer. *Invest Ophthalmol Vis Sci*. 2015;56:6095–6112.
21. Adhikari P, Zele AJ, Thomas R, Feigl B. Quadrant field pupillometry detects melanopsin dysfunction in glaucoma suspects and early glaucoma. *Sci Rep*. 2016;6:33373.
22. Obara EA, Hannibal J, Heegaard S, Fahrenkrug J. Loss of melanopsin-expressing retinal ganglion cells in severely staged glaucoma patients. *Invest Ophthalmol Vis Sci*. 2016; 57:4661–4667.
23. Valiente-Soriano FJ, Nadal-Nicolas FM, Salinas-Navarro M, et al. BDNF rescues RGCs but not intrinsically photosensitive RGCs in ocular hypertensive albino rat retinas. *Invest Ophthalmol Vis Sci*. 2015;56:1924–1936.
24. Vidal-Sanz M, Galindo-Romero C, Valiente-Soriano FJ, et al. Shared and differential retinal responses against optic nerve injury and ocular hypertension. *Front Neurosci*. 2017;11:235.
25. DeParis S, Caprara C, Grimm C. Intrinsically photosensitive retinal ganglion cells are resistant to N-methyl-D-aspartic acid excitotoxicity. *Mol Vis*. 2012;18:2814–2827.
26. Cui Q, Ren C, Sollars PJ, Pickard GE, So KF. The injury resistant ability of melanopsin-expressing intrinsically photosensitive retinal ganglion cells. *Neuroscience*. 2015;284:845–853.
27. Desai PV, Caprioli J. The treatment of normal-tension glaucoma. *Prog Brain Res*. 2008;173:195–210.
28. Kimura A, Namekata K, Guo X, Noro T, Harada C, Harada T. Targeting oxidative stress for treatment of glaucoma and optic neuritis. *Oxid Med Cell Longev*. 2017;2017:2817252.
29. Harada T, Harada C, Watanabe M, et al. Functions of the two glutamate transporters GLAST and GLT-1 in the retina. *Proc Natl Acad Sci U S A*. 1998;95:4663–4666.
30. Harada T, Harada C, Nakamura K, et al. The potential role of glutamate transporters in the pathogenesis of normal tension glaucoma. *J Clin Invest*. 2007;117:1763–1770.
31. Sano H, Namekata K, Kimura A, et al. Differential effects of N-acetylcysteine on retinal degeneration in two mouse models of normal tension glaucoma. *Cell Death Dis*. 2019;10:75.
32. Harada C, Kimura A, Guo X, Namekata K, Harada T. Recent advances in genetically modified animal models of glaucoma and their roles in drug repositioning. *Br J Ophthalmol*. 2019; 103:161–166.
33. Naskar R, Vorwerk CK, Dreyer EB. Concurrent downregulation of a glutamate transporter and receptor in glaucoma. *Invest Ophthalmol Vis Sci*. 2000;41:1940–1944.
34. Gherghel D, Mroczkowska S, Qin L. Reduction in blood glutathione levels occurs similarly in patients with primary-open angle or normal tension glaucoma. *Invest Ophthalmol Vis Sci*. 2013;54:3333–3339.
35. Manabe S, Gu Z, Lipton SA. Activation of matrix metalloproteinase-9 via neuronal nitric oxide synthase contributes to NMDA-induced retinal ganglion cell death. *Invest Ophthalmol Vis Sci*. 2005;46:4747–4753.
36. Namekata K, Kimura A, Kawamura K, et al. Dock3 attenuates neural cell death due to NMDA neurotoxicity and oxidative stress in a mouse model of normal tension glaucoma. *Cell Death Differ*. 2013;20:1250–1256.

Investigative Ophthalmology & Visual Science

37. Guo L, Salt TE, Maass A, et al. Assessment of neuroprotective effects of glutamate modulation on glaucoma-related retinal ganglion cell apoptosis in vivo. *Invest Ophthalmol Vis Sci*. 2006;47:626–633.
38. Manev H, Favaron M, Guidotti A, Costa E. Delayed increase of Ca2+ influx elicited by glutamate: role in neuronal death. *Mol Pharmacol*. 1989;36:106–112.
39. Kimura A, Namekata K, Guo X, Harada C, Harada T. Dock3-NMDA receptor interaction as a target for glaucoma therapy. *Histol Histopathol*. 2017;32:215–221.
40. Kuehn MH, Fingert JH, Kwon YH. Retinal ganglion cell death in glaucoma: mechanisms and neuroprotective strategies. *Ophthalmol Clin North Am*. 2005;18:383–395.
41. Kwon YH, Fingert JH, Kuehn MH, Alward WL. Primary open-angle glaucoma. *N Engl J Med*. 2009;360:1113–1124.
42. Ishikawa M. Abnormalities in glutamate metabolism and excitotoxicity in the retinal diseases. *Scientifica (Cairo)*. 2013;2013:528940.
43. Kimura A, Namekata K, Guo X, Noro T, Harada C, Harada T. Valproic acid prevents NMDA-induced retinal ganglion cell death via stimulation of neuronal TrkB receptor signaling. *Am J Pathol*. 2015;185:756–764.
44. Kimura A, Namekata K, Guo X, Harada C, Harada T. Neuroprotection, growth factors and BDNF-TrkB signalling in retinal degeneration. *Int J Mol Sci*. 2016;17:E1584.
45. Christensen I, Lu B, Yang N, Huang K, Wang P, Tian N. The susceptibility of retinal ganglion cells to glutamatergic excitotocity is type-specific. *Front Neurosci*. 2019;13:219.
46. Kitaoka Y, Kumai T. Modulation of retinal dopaminergic cells by nitric oxide. A protective effect on NMDA-induced retinal injury. *In Vivo*. 2004;18:311–315.
47. Vugler AA, Redgrave P, Semo M, Lawrence J, Greenwood J, Coffey PJ. Dopamine neurones form a discrete plexus with melanopsin cells in normal and degenerating retina. *Exp Neurol*. 2007;205:26–35.
48. Vaarmann A, Kovac S, Holmstrom KM, Gandhi S, Abramov AY. Dopamine protects neurons against glutamate-induced excitotoxicity. *Cell Death Dis*. 2013;4:e455.
49. Perez de Sevilla Muller L, Sargoy A, Rodriguez AR, Brecha NC. Melanopsin ganglion cells are the most resistant retinal ganglion cell type to axonal injury in the rat retina. *PLoS One*. 2014;9:e93274.
50. Berry M, Ahmed Z, Logan A. Return of function after CNS axon regeneration: lessons from injury-responsive intrinsically photosensitive and alpha retinal ganglion cells. *Prog Retin Eye Res*. 2019;71:57–67.
51. Li S, Yang C, Zhang L, et al. Promoting axon regeneration in the adult CNS by modulation of the melanopsin/GPCR signaling. *Proc Natl Acad Sci U S A*. 2016;113:1937–1942.
52. Schmidt TM, Alam NM, Chen S, et al. A role for melanopsin in alpha retinal ganglion cells and contrast detection. *Neuron*. 2014;82:781–788.
53. Ingham ES, Gunhan E, Fuller PM, Fuller CA. Immunotoxin-induced ablation of melanopsin retinal ganglion cells in a non-murine mammalian model. *J Comp Neurol*. 2009;516:125–140.
54. Galindo-Romero C, Jimenez-Lopez M, Garcia-Ayuso D, et al. Number and spatial distribution of intrinsically photosensitive retinal ganglion cells in the adult albino rat. *Exp Eye Res*. 2013;108:84–93.
55. Hughes S, Watson TS, Foster RG, Peirson SN, Hankins MW. Nonuniform distribution and spectral tuning of photosensitive retinal ganglion cells of the mouse retina. *Curr Biol*. 2013;23:1696–1701.
56. Kuze M, Morita T, Fukuda Y, Kondo M, Tsubota K, Ayaki M. Electrophysiological responses from intrinsically photosensitive retinal ganglion cells are diminished in glaucoma patients. *J Optom*. 2017;10:226–232.
57. Feigl B, Mattes D, Thomas R, Zele AJ. Intrinsically photosensitive (melanopsin) retinal ganglion cell function in glaucoma. *Invest Ophthalmol Vis Sci*. 2011;52:4362–4367.
58. Kankipati L, Girkin CA, Gamlin PD. The post-illumination pupil response is reduced in glaucoma patients. *Invest Ophthalmol Vis Sci*. 2011;52:2287–2292.
59. Gracitelli CP, Duque-Chica GL, Roizenblatt M, et al. Intrinsically photosensitive retinal ganglion cell activity is associated with decreased sleep quality in patients with glaucoma. *Ophthalmology*. 2015;122:1139–1148.
60. Kelbsch C, Maeda F, Strasser T, et al. Pupillary responses driven by ipRGCs and classical photoreceptors are impaired in glaucoma. *Graefes Arch Clin Exp Ophthalmol*. 2016;254:1361–1370.
61. Harada C, Namekata K, Guo X, et al. ASK1 deficiency attenuates neural cell death in GLAST-deficient mice, a model of normal tension glaucoma. *Cell Death Differ*. 2010;17:1751–1759.
62. Kimura A, Guo X, Noro T, et al. Valproic acid prevents retinal degeneration in a murine model of normal tension glaucoma. *Neurosci Lett*. 2015;588:108–113.

Investigative Ophthalmology & Visual Science